



This document is a postprint version of an article published in Science of The Total Environment© Elsevier after peer review. To access the final edited and published work see <https://doi.org/10.1016/j.scitotenv.2021.146664>

Document downloaded from:



1 **A high-resolution life cycle impact assessment model for continental** 2 **freshwater habitat change due to water consumption**

3 *Mattia Damiani*^{ac}, Philippe Roux^a, Eléonore Loiseau^a, Nicolas Lamouroux^b, Hervé Pella^b,*
4 *Maxime Morel^b, Ralph K. Rosenbaum^a*

5 ^a ITAP, INRAE, Montpellier SupAgro, Univ Montpellier, ELSA Research Group and ELSA-
6 PACT Industrial Chair, Montpellier, France

7 ^b INRAE Lyon, UR RiverLy, Villeurbanne, France

8 ^c Department of Environmental Sciences, Informatics and Statistics, Ca' Foscari University of
9 Venice, Mestre-Venezia, Italy

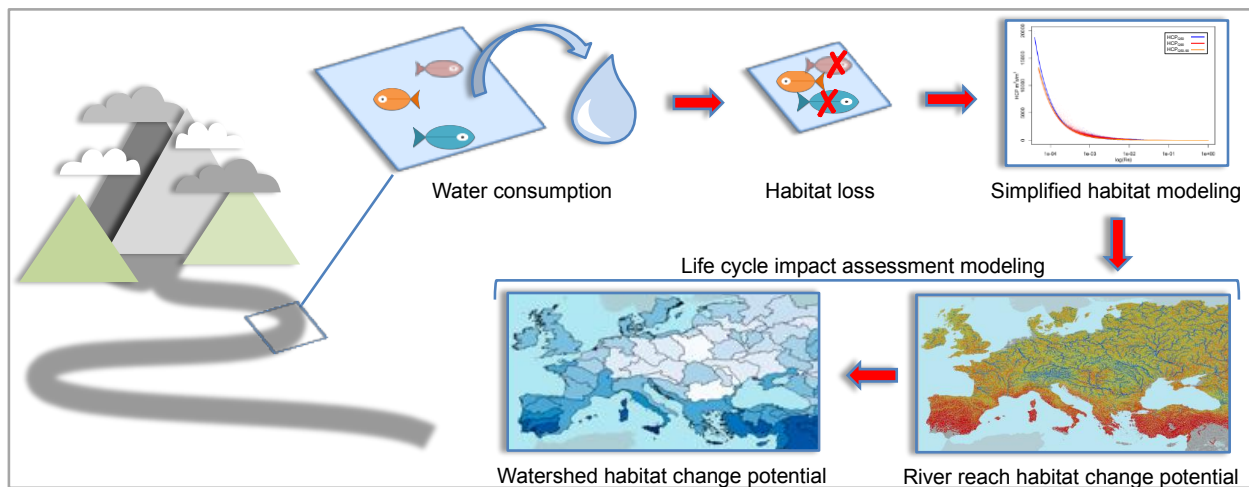
10 *Corresponding author: damianimtv@gmail.com

11 **ABSTRACT**

12 Global value chains and climate change have a significant impact on water resources and
13 increasingly threaten freshwater ecosystems. Recent methodological proposals for life cycle
14 impact assessment (LCIA), evaluate water use impacts on freshwater habitats based on river
15 hydraulic parameters alterations. However, they are limited to French rivers due to lack of global
16 data and models. On this basis, this article proposes an approach to compute regionalized
17 characterization factors for modeling river habitat change potential (HCP) induced by water
18 consumption, potentially applicable worldwide. A simplified model is developed for fish guilds
19 and invertebrates. Based on French datasets, it establishes a relationship between HCP and river
20 hydraulic parameters. A methodology to derive discharge and hydraulic geometry at the reach
21 scale is proposed and applied to European and Middle Eastern rivers below 60°N latitude.
22 Regionalized HCPs are calculated at the river reach scale and aggregated at watershed. Then, the

23 impact of agricultural water use in contrasted European and Middle Eastern countries is evaluated
24 comparing the outcomes from the HCP and the Available Water Remaining (AWARE) models at
25 the national scale, considering water supply mix data. The same analysis is carried out on selected
26 river basins. Finally, result consistency, uncertainty and global applicability of the overall
27 approach are discussed. The study demonstrates the reproducibility of the impact model developed
28 for French rivers on any hydrographic network where comparable ecological, hydrological and
29 hydraulic conditions are met. Furthermore, it highlights the need to characterize impacts at a higher
30 spatial resolution in areas where HCP is higher. Large scale quantification of HCP opens the way
31 to the operationalization of mechanistic LCIA models in which the habitat preferences of
32 freshwater species are taken into account to assess the impacts of water consumption on
33 biodiversity.

34 GRAPHICAL ABSTRACT



35

36 KEYWORDS

37 Life cycle impact assessment, water consumption, freshwater habitat, biodiversity

38 **ABBREVIATIONS**

39 LCA, life cycle assessment; LCIA, life cycle impact assessment; CF, characterization factor; FF,
40 fate factor; EF, effect factor; HCP, habitat change potential; Q, river discharge; CWU,
41 consumptive water use; HS, habitat suitability; WUA, weighted usable area; Re, Reynolds number;
42 W, river width ; HB, HydroBASINS; WSmix, water supply mix.

43 1. INTRODUCTION

44 Human interaction with water systems in the Anthropocene is being expressed through the
45 pervasive alteration of the global water cycle. This stimulated the contextualization of watershed
46 scale management paradigms under a global-scale perspective leading to the production of an
47 increasing amount of knowledge about worldwide freshwater resource availability and
48 exploitation (Vörösmarty et al., 2013). Water use for human activities and the exportation of water-
49 hungry products in globalized supply chains (Dalin et al., 2017; Moran and Kanemoto, 2017),
50 besides the consideration of the geopolitical implications of global water cycle modification, call
51 for a better understanding of effective and potential consequences on water-dependent ecosystems.

52 More than 50% of the major river basins on Earth are threatened by pollution and disturbance
53 of natural flow regimes, with damming, river fragmentation and consumptive water use among the
54 main causes of biodiversity loss (Vörösmarty et al., 2010). Notwithstanding, estimations of global
55 river threats and biodiversity status are often partial, since small streams are barely captured by
56 global statistics, despite being generally more sensitive to anthropic pressures. High resolution
57 global surface water availability models are nowadays of great importance (Pekel et al., 2016) and
58 the refinement of methods to assess freshwater requirements of ecosystems and biodiversity is
59 needed (Janse et al., 2015; Pastor et al., 2014).

60 Life cycle assessment (LCA) is a service and product-oriented approach to global-scale analysis
61 of supply chains for various impact categories, including water use. Impact indicators can quantify
62 damage on the environment at the end of a cause-effect chain (i.e. endpoint impact on resources,
63 human health, and ecosystem quality), or describe environmental mechanisms occurring prior to
64 the endpoint (i.e. midpoint). Characterization factors are developed to convert inventory data (e.g.
65 m³ of water consumed per unit of product) to the corresponding impact indicators. Depending on

66 the type of impact, characterization factors may consider physical change of local environmental
67 conditions caused by a stressor (fate factor), the exposure of sensitive targets (exposure factor),
68 and any related adverse effects (effect factor).

69 AWARE, a consensus model for water use impact assessment in LCA, proposed by the UNEP-
70 SETAC Life Cycle Initiative working group on water use in LCA (WULCA), includes
71 environmental water requirements (EWR) in the quantification of available water remaining for
72 life cycle impact assessment (LCIA) midpoint characterization (Boulay et al., 2018). Pfister et al.
73 (2009) developed endpoint characterization factors for freshwater consumption impacts on net
74 primary productivity (NPP) of vascular plants as a proxy for species loss. The model proposed by
75 Verones et al. (2017, 2013a, 2013b) quantifies potential biodiversity impacts for birds, amphibians,
76 reptiles and mammals in wetlands. Existing LCIA models for riverine species based on species-
77 discharge relationships (Hanafiah et al., 2011; Tendall et al., 2014) have limitations in capturing
78 changes in river communities because they do not consider the different responses that species
79 adapted to different habitats have to river flow reduction or increase (Damiani et al., 2019, 2018).
80 All these models address furthermore the need for regionalized characterization factors, further
81 raised, for instance, with recent LCA application at the territorial scale (Loiseau et al., 2018;
82 Nitschelm et al., 2016), and should ultimately be coupled with spatially explicit information on
83 water supplies (Leão et al., 2018).

84 Modeling at watershed spatial resolution is consistent with widely employed water management
85 practices for river ecosystems protection (Palmer et al., 2009). LCIA should therefore aim at
86 providing global, regionalized models based on mechanistic approaches applied at watershed and
87 sub-watershed levels. At present, no operational mechanistic model to assess water consumption
88 impacts on stream ecosystems is available at the global scale (Damiani et al., 2018; Núñez et al.,

89 2016). A high-resolution midpoint impact indicator of habitat change potential (HCP) based on
90 freshwater physical habitat suitability for fish species, fish guilds and benthic macroinvertebrates
91 has recently been proposed (Damiani et al., 2019). HCP quantifies the potential change in available
92 habitat quantity on a river and watershed scale as a result of water consumption, taking into account
93 the habitat preferences of freshwater fish and invertebrate species. However, the model is only
94 applicable to the French river network and a worldwide extension needs to be investigated. The
95 present study builds on this approach proposing a method for the development of characterization
96 factors for water consumption impacts on freshwater instream ecosystems, to be implemented
97 worldwide.

98 The availability of global data required to apply the habitat suitability equations adopted in the
99 local French mechanistic approach is first evaluated. Based on available databases, missing
100 variables are identified, namely topographical, hydrological and hydraulic. The high-resolution
101 HCP model is then simplified to reduce complexity of input variables and to adapt to their
102 availability. Variables are subsequently calculated from existing models to allow implementation
103 outside France. An application of the new HCP model (referred to as generalized or global HCP
104 throughout the article) on the European continent and the Middle East is then demonstrated and
105 discussed. Characterization factors are calculated at the river reach scale and then aggregated at
106 watershed scale. Results are compared with those of the original local model applied in France and
107 a case study on European agricultural production is presented to show potential similarities and
108 dissimilarities between the generalized HCP model and the AWARE model, since it is the only
109 (proxy-) midpoint method actually including water demand for river ecosystems in the
110 characterization and providing regionalized characterization factors for watersheds worldwide.

111 2. MATERIALS AND METHODS

112 2.1 Habitat change potential at river reach scale

113 Characterization factors based on HCP were computed from Equation (1) (taken from Damiani
114 et al., 2019), where CF_i is the characterization factor at river reach i . FF is the fate factor calculated
115 as the ratio between the difference in river discharge dQ (m^3/s) for each cubic meter of
116 consumptive water use $dCWU$ and it is assumed to be equal to 1 (Hanafiah et al., 2011). EF is the
117 effect factor represented by habitat change potential HCP in $m^2 s/m^3$ (change in m^2 suitable habitat
118 quantity induced by river discharge alteration in m^3/s), then $CF = HCP$. In Damiani et al. (2019),
119 the authors calculated HCP from seventeen multivariate habitat suitability equations
120 corresponding to four fish guilds with different habitat preferences, eight fish species where some
121 of them at different stage of development (i.e. alevin, juvenile, adult; Lamouroux and Capra,
122 2002), and a generic equation for benthic macroinvertebrates.

$$123 \quad CF_i = FF_i \cdot EF_i = \frac{dQ_i}{dCWU_i} \cdot HCP_i \quad (1)$$

124 HCP values were aggregated at reach scale to facilitate their use in LCIA, resulting in two
125 indicators, one of which gathers guilds and invertebrates HCPs. For a global application of the
126 model, we adopted the latter since we assume it summarizes a sufficiently large spectrum of habitat
127 preferences without referring necessarily to particular species for which the distribution would be
128 uncertain (see Table S1 in Supporting Information – SI – for guilds characteristics). Nevertheless,
129 in the aggregated characterization factor, fish species favoring shallow and running waters
130 dominate the overall characterization factor since their habitat is more sensitive to water quantity
alteration.

131 Data availability at the global scale is a major constraint for a worldwide application of the HCP
 132 model. In Table 1 input variables of the local HCP model are listed.

133 **Table 1.** Variables required to run the HCP model of Damiani et al. (2019)

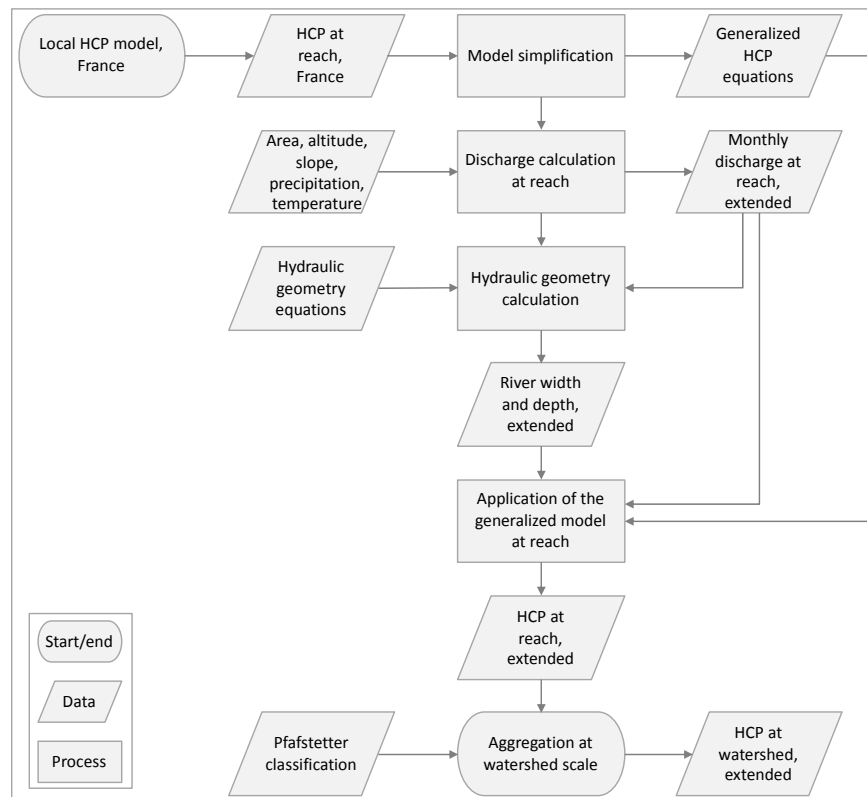
| Reach Variable | Unit |
|---|-------------------|
| Upstream catchment area (A) | km ² |
| Slope (S) | % |
| Strahler order (O) | |
| Width (calculated from Q , A , S and O) | m |
| Depth (calculated from Q , A , S and O) | m |
| Substrate particle diameter | mm |
| Inter-annual average discharge (\bar{Q}) | m ³ /s |
| Inter-annual natural Median daily discharge ($Q50$) | m ³ /s |
| Inter-annual low flow discharge daily percentile ($Q90$), over which daily discharge is 90% of the time | m ³ /s |

134

135 The model applied in France in Damiani et al. (2019) is based on the French theoretical
 136 hydrographical network (RHT, Pella et al., 2012) which has a resolution of the order of meters and
 137 provides all input variables needed to quantify habitat change potentials. Data in Table 1 with the
 138 same spatial precision are currently not available globally. The products derived from the
 139 HydroSHEDS database at 15 arc-sec (≈ 500 m at the equator) represent, to our knowledge, the best
 140 available option in terms of spatial resolution of river segments and global coverage (Lehner and
 141 Grill, 2013), but hydrological, hydraulic and topographical information are seldom associated to
 142 such datasets with the same accuracy as in the RHT network.

143 **2.2 Modeling regionalized HCPs worldwide**

144 The difficulty in deriving data at the river reach scale for substrate composition and especially
 145 for flow magnitudes hinders the global parameterization of HCP (e.g. flow exceedance probability
 146 for Q_{50} and Q_{90} was calculated from daily streamflow data in the RHT network). For this reason,
 147 a generalization of the local HCP model was developed to reduce the data requirements shown in
 148 Table 1. Subsequently, input variables of the simplified model were calculated for European and
 149 Middle Eastern river segments and the results of HCP characterization at reach were aggregated
 150 at watershed scale (Figure 1).



151
 152 **Figure 1.** Logical approach for the characterization of habitat change potential at the global scale,
 153 demonstrated on European and Middle Eastern rivers

154 2.3 Extrapolation of a generalized HCP model

155 Habitat change potential was quantified on French rivers for Q_{50} and Q_{90} , representing median
156 and low flows respectively. The discharge-dependent input variable of the LCIA model, which is
157 directly altered by water consumption, is the Reynolds number Re , calculated as the ratio between
158 river discharge Q and the product of water viscosity ν (considered equal to 10^{-6} m²/s) and river
159 width W . To avoid working with high values, Re is multiplied by 10^{-7} (Damiani et al., 2019;
160 Lamouroux and Capra, 2002; Lamouroux and Souchon, 2002). Non-linear least squares analysis
161 was used to fit a power model to HCP results for Re at Q_{50} and Q_{90} (Equations (2) and (3)). Model
162 fitting was carried out in R (R Core Team, 2016; RStudio Team, 2016). When modeling HCP for
163 the world's rivers, defining where and in which period of the year median and low flow conditions
164 occur is not straightforward. To solve this, an equation was derived by fitting the model on Q_{50}
165 and Q_{90} HCPs together, ranging from -1.8 to 22 396.3 m² s/m³ (Equation (4)). The residuals root-
166 mean-squared errors (RMSE) indicate that the average spread of sample data around the regression
167 line is lower than 0.5% of the HCP range for the three equations and can thus provide a measure
168 of the goodness of fit of the simplified models.

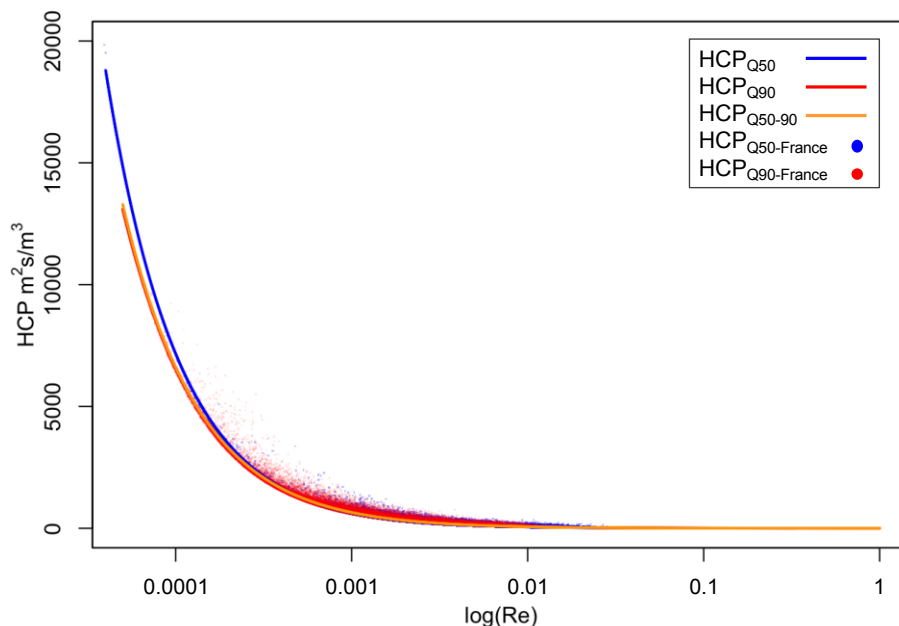
$$HCP_{Q_{50}} = 0.439 \cdot \left(\frac{Q_{50}}{\nu \cdot W_{50}} \right)^{-1.053} \quad \text{RMSE} = 50 \quad (2)$$

$$HCP_{Q_{90}} = 0.669 \cdot \left(\frac{Q_{90}}{\nu \cdot W_{90}} \right)^{-0.998} \quad \text{RMSE} = 108 \quad (3)$$

$$HCP_{Q_{50-90}} = 0.614 \cdot \left(\frac{Q}{\nu \cdot W} \right)^{-1.008} \quad \text{RMSE} = 86 \quad (4)$$

169 In case precise determination of flow exceedance probability is available at the scale of a river
170 segment, Equation (2) and (3) are preferable, otherwise, and for the present study, the $HCP_{Q_{50-90}}$
171 equation was used to calculate characterization factors in Europe and the Middle East.

172 Nonetheless, as shown in Figure 2, results of the three models are not dissimilar, with HCP_{Q90} and
173 HCP_{Q50-90} almost overlapping for high HCP values, and the three curves converging as flow
174 increases.



175
176 **Figure 2.** Power models describing HCP variation with Reynolds number. Curves fitted on HCP
177 values at $Q50$ and $Q90$ in French rivers

178 **2.4 HCP global model's input variables and application at reach scale**

179 As demonstrated by the simplified HCP Equations (2), (3), (4), HCP can be calculated globally
180 from river discharge and width. At present, global flow data estimated at watershed scale are
181 available (WaterGAP, Alcamo et al., 2003; Döll et al., 2003), a global dataset have been recently
182 derived from WaterGAP for discharge at river segment scale (Linke et al., 2019), but yet no $Q50$
183 and $Q90$ data are available. A regression model to estimate mean, annual streamflow was recently
184 proposed based on empirical data from globally distributed gauging stations (Equation (5), adapted
185 from Barbarossa et al., 2017).

$$Q_{it} = 10^{9.066} \cdot A_i^{1.018} \cdot H_i^{-0.509} \cdot S_i^{0.464} \cdot P_{it}^{2.070} \cdot 10^{-0.038 \cdot T_{it}} \quad (5)$$

186 To improve temporal resolution of existing datasets, in this study, this model was used to
 187 calculate discharge at reach i and month t from the input parameters, listed in Table 2 along with
 188 the data sources used.

189 **Table 2.** Input data for discharge calculation at river reach (adapted from Barbarossa et al., 2017)

| Variable | Unit | Data source | Reference | Resolution | |
|-------------------|----------------|---|------------------------|------------|----------|
| | | | | Spatial | Temporal |
| Drainage area (A) | m ² | A simple global river bankfull width and depth database | Andreadis et al., 2013 | 15 arc-sec | - |
| Altitude (H) | m | HydroSHEDS | Lehner and Grill, 2013 | 15 arc-sec | - |
| Slope (S) | (°) | HydroSHEDS (calculated) | | | |
| Precipitation (P) | m/s | WorldClim | Fick and Hijmans, 2017 | 30 arc-sec | Month |
| Temperature (T) | °C | WorldClim | | | |

190
 191 Drainage area was taken from the hydraulic geometry dataset of Andreadis et al. (2013) where
 192 catchment surface values are associated to each river segment present in the HydroSHEDS 15 arc-
 193 sec hydrographic network with river segments in desert areas masked out. Minimum, maximum
 194 and average altitudes were attributed to each segment based on the HydroSHEDS digital elevation
 195 model (DEM) at 15 arc-sec. Reach length was also calculated to be able to derive average slope in
 196 degrees according to Equation (6). A factor of 0.5 which is half of the resolution of the DEM, was
 197 added to Equation (6) to avoid zero values of slope that would result in zero discharge. It was
 198 therefore implicitly assumed that with a slope equal to zero, river reach discharge is fed by
 199 upstream water inertial flow.

$$Slope_i = \arcsin\left(\frac{H_{i\ max} - H_{i\ min} + 0.5}{Length_i}\right) \cdot \left(\frac{180}{\pi}\right) \quad (6)$$

200 Precipitation and temperature were derived from the WorldClim database at 30 arc-sec
 201 resolution. Considering that the dataset provides climatic data with a monthly resolution,
 202 streamflow values (Q) were calculated for each month t , substituting monthly values of P and T in
 203 Equation (5). All spatial geoprocessing was carried out using SAGA and QGIS (Conrad et al., 2015;
 204 Quantum GIS Development Team, 2017).

205 Currently no global databases are available including width (W) at the reach scale for monthly
 206 discharge values. However, hydraulic geometry relationships between discharge, width, depth and
 207 velocity have been described extensively and, with some approximation depending on the chosen
 208 method, can be computed by models that remain valid worldwide (Leopold and Maddock, 1953;
 209 Park, 1977; Rhodes, 1978). In particular, Morel et al. (2020) collected most of the hydraulic
 210 geometry data available at the scale of stream reaches. They found high intercontinental similarity
 211 in hydraulic geometry models between France and New Zealand, suggesting that their results can
 212 be applied globally. Here, to provide global hydraulic geometry relationships that represent
 213 variations in width W in space (among reaches) and time (with discharge Q), we used a
 214 combination of the “downstream” (in space) and “at-a-station” (in time) formulations of hydraulic
 215 geometry of Leopold and Maddock (1953), following the approach of Lamouroux and Souchon
 216 (2002) and Morel et al. (2020) (Equation (7)):

$$W_{it} = \left[a_d \cdot \bar{Q}_i^{b_d} \right] \cdot \left[\frac{Q_{it}}{\bar{Q}_i} \right]^b \quad (7)$$

217 where a_d and b_d are the “downstream” hydraulic geometry parameters for width, and b is the “at-
 218 a-station” exponent that describes variations with discharge. We fitted these three parameters to

219 the data from 1304 reaches of France and New Zealand available in Morel et al. (2020), giving a_d
220 $= 7.482$, $b_d = 0.477$, and $b = 0.148$.

221 To demonstrate the applicability of the global HCP model at the reach scale, habitat change
222 potential was quantified on 449 508 river segments covering Europe and the Middle Eastern
223 regions. Since all variables were calculated on rivers derived from SRTM-based datasets (NASA's
224 Shuttle Radar Topography Mission), such as HydroSHEDS, the dataset is limited to rivers below
225 60°N latitude (taken from Andreadis et al., 2013). The original model developed for French rivers
226 has limited relevance for high flow periods and, in consequence, the derived global model as well.
227 Global HCP was calculated using Equation (4) on a monthly basis because for a large-scale
228 application it is not possible to determine high, median and low flows in regions with different
229 climate and hydrological conditions. For this reason, it is not possible to exclude some months a
230 priori from the characterization. This choice is further discussed in section 4.

231 **2.5 HCP aggregation at watershed scale**

232 Regionalization of characterization factors is necessary because in LCA it is difficult to obtain
233 the detail of local water withdrawal and release, especially for background activities and pre-
234 compiled processes in existing databases, where only average national values are usually available.
235 With regard to the HCP model, the optimal spatial resolution should be a trade-off between habitat
236 model uncertainties at the local scale and HCP spatial variability (Damiani et al., 2019). HCP
237 modeling at watershed level could be the best option in this sense. Reach HCPs were thus
238 aggregated according to watershed boundaries defined in the HydroBASINS dataset (Lehner and
239 Grill, 2013) at level 03 and 04 (HB03, HB04), assigning to each river segment the Pfafstetter codes
240 corresponding to the respective watersheds. The formula used for the aggregated characterization

241 factor at watershed (CF_{wt}) was taken from Damiani et al. (2019) where the ratio between individual
 242 length of river segments and the total length of all catchment rivers is the weighting factor for
 243 HCPs calculated at reach that are subsequently summed up in an aggregated score. However, since
 244 high stream order rivers are not included in the European database (Strahler order 1 and part of
 245 Strahler order 2), we chose to also aggregate based on average river water volume V (m^3) per
 246 month t residing in each river segment, as in Equation (8):

$$CF_{wt} = FF_{wt} \cdot EF_{wt} = \frac{dQ_{wt}}{dCWU_{wt}} \cdot \sum_{i=1}^n HCP_{it} \cdot \frac{V_{it}}{\sum_{i=1}^n V_{it}} \quad (8)$$

247 where water volume is the product of width W , depth D and length. It was therefore necessary
 248 to calculate monthly river depth D , by means of Equation (9), following the same reasoning of
 249 Equation (7):

$$D_{it} = \left[c_d \cdot \bar{Q}_i^{f_d} \right] \cdot \left[\frac{Q_{it}}{\bar{Q}_i} \right]^f \quad (9)$$

250 where c_d and f_d are the “downstream” hydraulic geometry parameters for depth, and f is the “at-
 251 a-station” exponent ($c_d = 0.340$, $f_d = 0.259$, $f = 0.292$ from the data in Morel et al., 2020). The
 252 difference between length and volume weighting is that the first method implies equal weight for
 253 all reaches in the drainage basin and missing high order streams would likely bias the result of the
 254 characterization. In the latter the quantity of water that a river provides to the drainage basin is the
 255 weighting factor. This implies the assumption that the water consumed within a watershed has
 256 higher probability of being withdrawn from rivers with higher volume of available water.

257 After aggregation, the outputs of the generalized model were compared to those resulting from
 258 the French model to test results consistency. Four watersheds entirely included into French borders
 259 were taken into account. $Q90$ and August characterization factors were compared for the local and
 260 the generalized model respectively. According to the data used for HCP modeling in this study,

261 August is generally the driest month of the year, with exceptions such as in glacier-fed streams. It
262 is therefore more likely to have low flows (Q_{90}) occurring in this period of the year.

263 **2.6 Application to European agricultural water use**

264 The global, regionalized HCP model was applied to a case study to discuss its usability and
265 interest for LCA. Agriculture alone is responsible for 70% of global water withdrawals (UNESCO
266 and UN-Water, 2020), 40% in Europe (European Environment Agency, 2018). The impact of 1
267 m^3 water consumption for agricultural use according to available agricultural water supply mixes
268 was assessed (WSmix, Leão et al., 2018). Calculations were made for selected European countries
269 with agricultural water consumption greater than 1 000 million m^3 /year, including Turkey and
270 Azerbaijan (SI, Table S4). Since the HCP model applies to surface water habitats, impact is
271 calculated for the share of surface water in the WSmix. This encompasses generic surface water
272 consumption data, spring water, inter-basin transferred water and reservoirs. Although, artificial
273 impoundments per se are not directly covered by the HCP model which is more sensitive to habitat
274 variation in streams, reservoirs were included because the differentiation between the two types of
275 water sources was available for a few countries only, while in most cases the information is hidden
276 in generic surface water use. Moreover, reservoir water is often used to maintain river flow in dry
277 periods or when water demand is higher, and in this case can thus be considered as stream water,
278 except that abstraction is delayed in time. National annual average HCPs were calculated from
279 watershed HCPs of each country and compared with the AWARE CFs for agriculture at the same
280 spatial and temporal resolution. AWARE quantifies available water remaining after the demand
281 of humans and aquatic ecosystems has been met (Boulay et al., 2018). Since Spain had the best
282 detail on watershed and sub-watershed WSmixes among selected countries in Leão et al. (2018),

283 comparisons between HCP and AWARE were also made at watershed scale for Spanish river
284 basins to discuss spatial scale choices for HCP characterization (SI, Table S5).

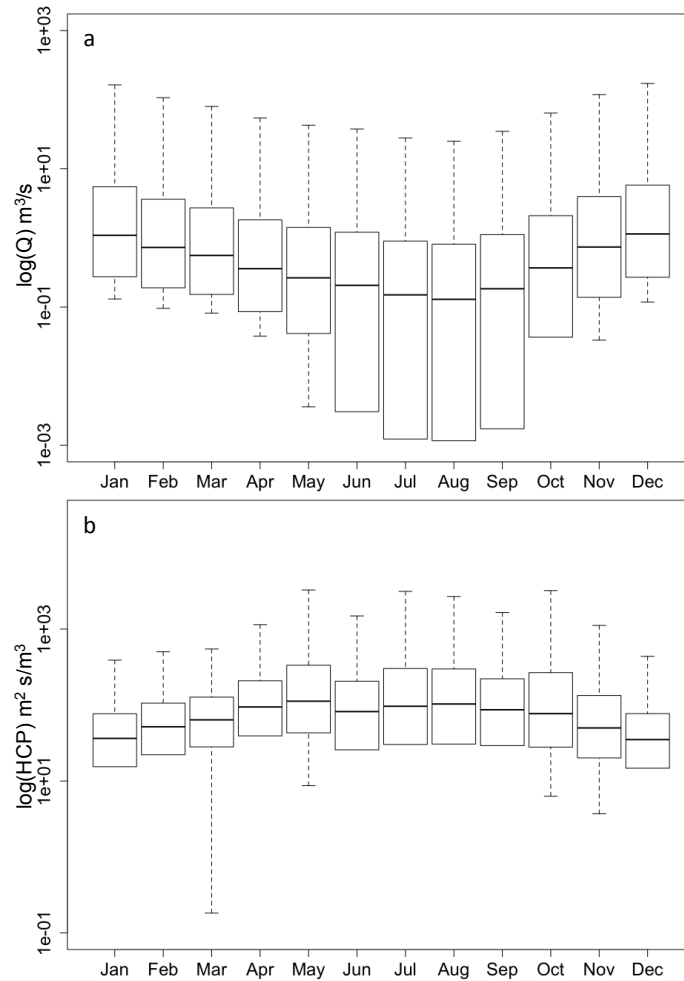
285 **3. RESULTS AND DISCUSSION**

286 **3.1 HCP modeling at reach and watershed scale**

287 The mean annual streamflow model applied to European rivers and adjusted with monthly
288 climatic data, allows estimating the seasonal variability in river discharge along the year, deriving
289 from rainfall and temperature. Figure 3 represents the detail of monthly Q and HCP distribution in
290 the selected rivers excluding extreme values (R robustbase package for skewed distributions,
291 Hubert and Vandervieren, 2008). Outliers are not represented because of the size of the data sample
292 and the high variability of European and Middle Eastern climatic conditions and river regimes.
293 The latter would result in extremely low discharge values for small rivers in dry periods (e.g. small
294 streams in the Mediterranean region and the Middle East) and six orders of magnitude greater
295 flows in big rivers during wet months (e.g. in major rivers of continental Europe). For each month,
296 streamflow distribution is right skewed with maximum median and average values of 1.03 m³/s
297 and 61.58 m³/s respectively (both in December), reflecting the predominance of small streams in
298 the modeling dataset.

299 A reduction in river discharge in dry months is associated to a lower average Reynolds number
300 in river reaches and therefore to higher habitat change potential for those habitats more likely to
301 be damaged by water deprivation (shallow and well oxygenated running waters). Figure 3 confirms
302 the lower availability of water in summer months and the associated higher habitat sensitivity to
303 water consumption. In wet season, indicatively from November to April, 95% of European rivers
304 included in the study fall between discharge values of 0 and 299.6 m³/s. From May to October Q

305 is between 0 and 37.4 m³/s. The derived HCP is comprised between 0 and 4 070.9 m² s/m³ in wet
306 months and between 0 and 13 352.9 m² s/m³ in dry season (see SI, Tables S2 and S3).



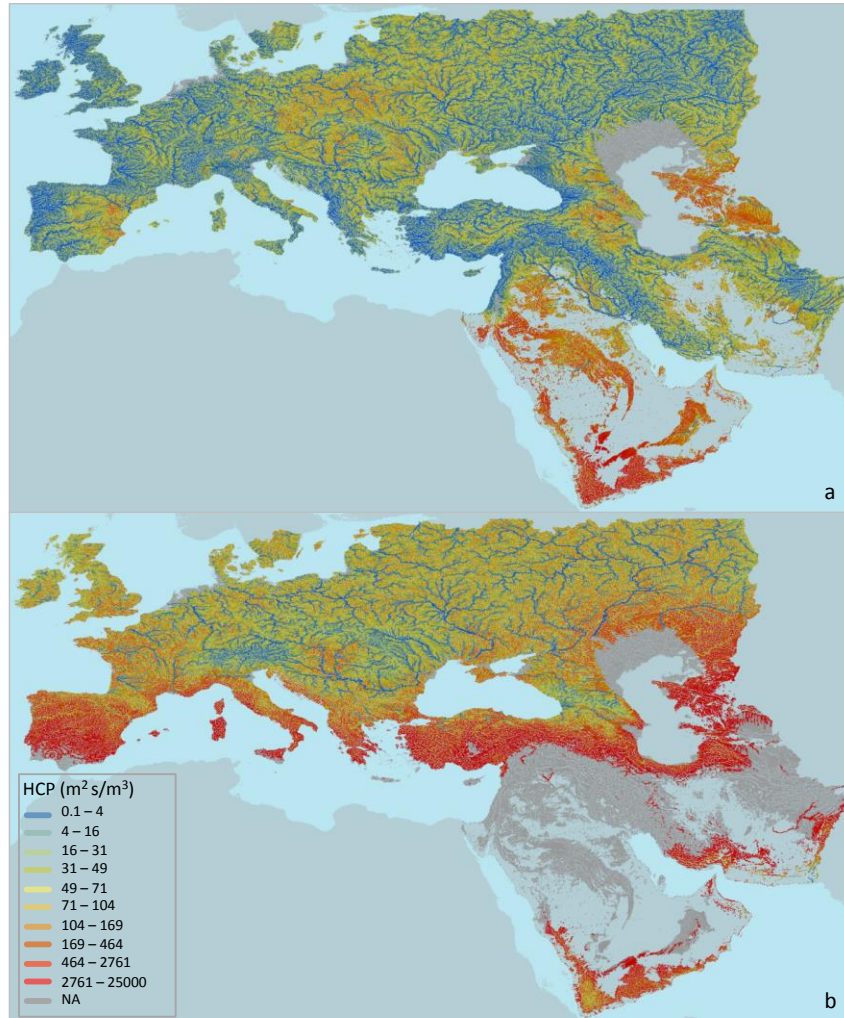
307
308 **Figure 3.** Monthly discharge Q in European rivers (a) and HCP characterization factors
309 distribution (b)

310 Figure 4 illustrates HCP in European and Middle Eastern reaches in January and July.
311 Characterization factors of the other months are shown in SI, Figure S1. The results highlight an
312 increase of habitat change potential in dry season, especially in the Mediterranean region and
313 diffusely in arid areas of the Middle East and the Caspian Sea (Kazakhstan, Turkmenistan, Iran).
314 Dark grey-shaded river segments are those where the HCP model cannot be applied for different

315 reasons. Overall, HCP greater than $25\,000\text{ m}^2\text{ s/m}^3$ were considered outside the validity range of
316 the habitat model, according to the scores obtained in the local HCP model (Damiani et al., 2019)
317 from which the generalized model was derived. The maximum amount of such values was
318 observed in August for 44 860 river segments corresponding to 10% of the total. These streams
319 are located essentially in the Middle East and in desert regions, corroborating the non-applicability
320 of the model since it has been developed from river ecosystems pertaining to different climatic
321 regions and hydrological conditions.

322 A characterization factor is also not quantifiable in rivers where discharge is equal to 0.
323 According to the formula used to quantify Q , described in section 2, this may happen for two
324 reasons. The first one is for reaches that are not sustained by runoff fed from rainfall and that cease
325 to flow periodically (Figure 4b). In the modeled dataset this applies to 12.8% of river segments
326 maximum in September, mostly in arid and desert areas. In this case, the global HCP model is not
327 applicable since rivers dry out and no habitat is present. Moreover, it should be considered that the
328 uncertainty deriving from applying the characterization model on non-perennial rivers, such as
329 those represented in Figure 4a and masked out in Figure 4b in the Arabian Peninsula, is high. In
330 Figure 3, the peaks in HCP values in May and October is due to the fact that precipitation and thus
331 a modest value of discharge can be attributed to these rivers at the two boundaries between wet
332 and dry season, resulting in high HCP extremes (SI, Table S3 and Figure S1). However,
333 ecosystems of intermittent and ephemeral rivers are still the subject of extensive research (Leigh
334 et al., 2016) and, although potential physical habitat availability can be represented by the HCP
335 indicator, these streams are characterized by specific ecological mechanisms that cannot be
336 exhaustively described by the HCP model.

337 Discharge, and therefore HCP, could not be attributed also in river segments where the altitude
338 is equal to or lower than 0. These conditions are distinctive in estuarine and brackish areas that are
339 out of the scope of the HCP model. Even if fish species are not taken into account, impact of water
340 use on wetland ecosystems is covered by the models proposed by Verones et al. (2013a, 2013b)
341 which can be therefore complementary to our model.

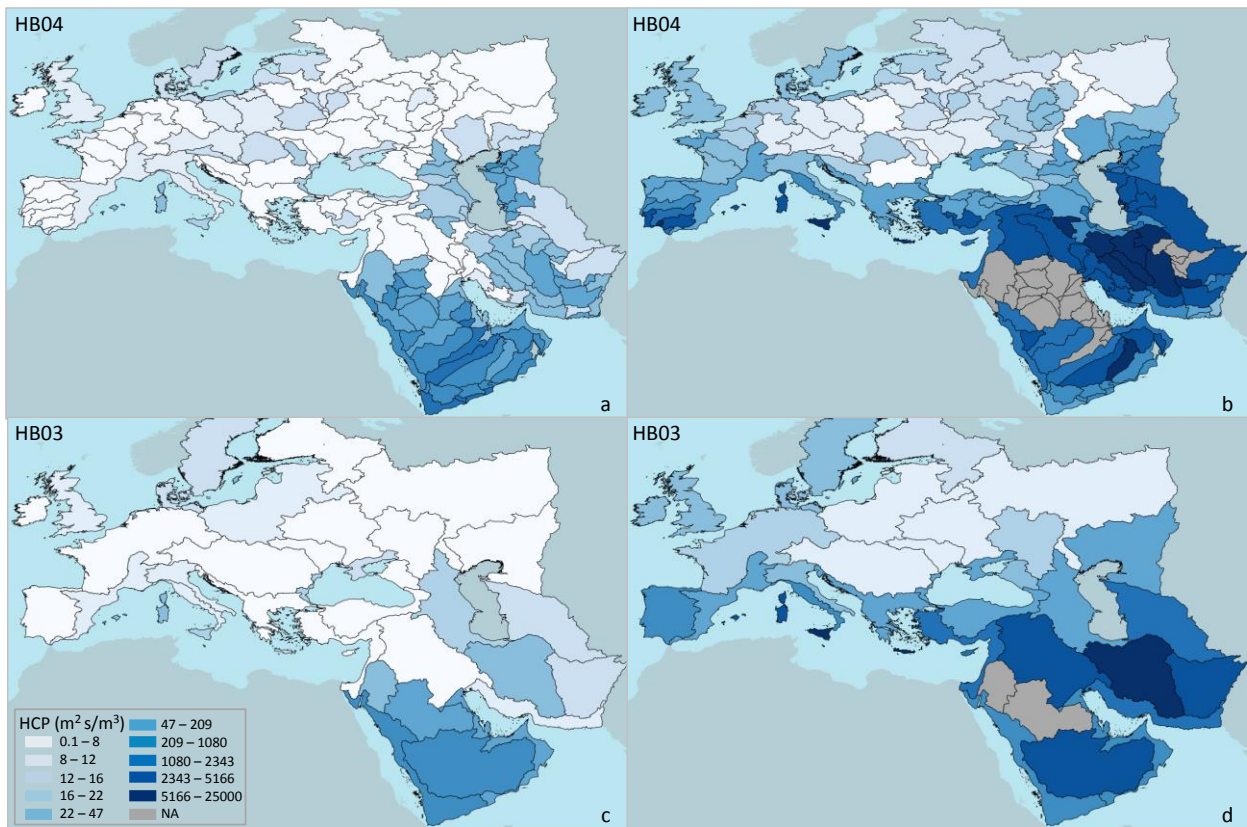


342

343 **Figure 4.** Habitat change potentials in a) January and b) July

344 **3.2 Watershed characterization factors**

345 Aggregated characterization factors at watershed level reflect the outcomes of reach-scale HCP
346 with higher values during summer months in Mediterranean and arid regions for both aggregation
347 formulas tested on river lengths and volumes (the latter applied in Figure 5). Higher level
348 aggregation at HB03 averages the impact of smaller, contiguous sub-watersheds resulting overall
349 in lower HCP scores. Outcomes of both aggregation methods highlight a decrease of HCP values
350 when volume weighting is performed, as shown in Table 3.



351
352 **Figure 5.** Aggregation of reach-scale HCPs based on water volumes in a) January, HB04; b) July,
353 HB04; c) January, HB03; d) July, HB03

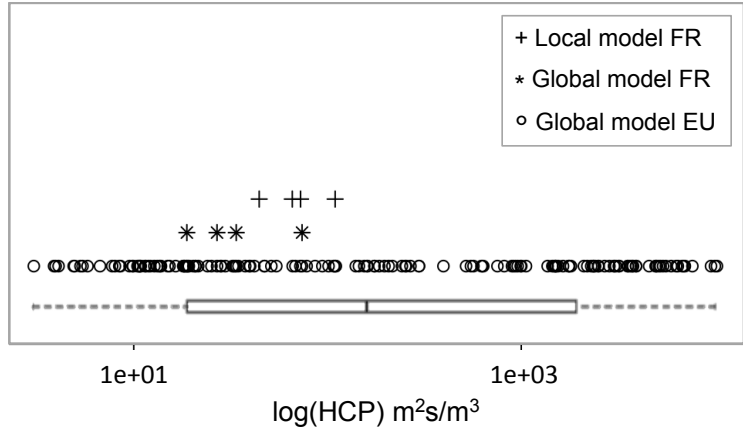
354 **3.3 Consistency analysis**

355 In French watersheds at HB04, the comparison between aggregated HCPs on length in the local
356 model and in the present study showed six times smaller HCP deriving from the generalized model.
357 This is due to the fact that small, high order streams are missing in the European database (Strahler
358 orders 1 and 2 with higher HCP) but not in the detailed French RHT network. Moreover, the
359 relative magnitudes of the characterization value between watersheds are different in both models.
360 Aggregation on volume is therefore preferable as the relationships between watersheds remain
361 consistent and the ratio between local and generalized CFs is decreased to two times when high
362 order streams are taken into account. Recalculating aggregated CFs from the local French model
363 excluding river segments with Strahler order 1 and 2, resulted in further reducing the discrepancy
364 with global HCP scores for France, showing very close characterization factors (Table 3). In
365 absolute terms, these differences are far below the root-mean-squared error associated to the
366 generalized model in equation (4). Uncertainty resulting from deriving a generalized model from
367 a spatially limited one, can be attenuated if at-reach characterization factors are aggregated at
368 watershed scale. Notwithstanding, on a continental scale the deviation of generalized CFs from
369 local CFs is negligible, as demonstrated in Figure 6 for aggregated HCPs.

370 **Table 3.** Comparison between aggregated HCP scores ($m^2 s/m^3$) for French watersheds from the
 371 local model (Q90) and the generalized, global characterization model applied to European river
 372 basins (July)

| Pfaf | HCP _l | | HCP _v | | | | HCP _l | HCP _v | HCP _v | HCP _v | FR | EU |
|------|------------------|-------|------------------|------------|------------|-----------|------------------|------------------|--------------------|--------------------|--|--|
| | FR | EU | FR | FR St>1 | FR St>2 | EU | FR/EU | FR/EU | FR/EU (FR St>1) | FR/EU (FR St>2) | HCP _l / HCP _v | HCP _l / HCP _v |
| 2321 | 710.2 | 144.4 | 65.8 | 34.0 | 25.1 | 33.8 | 4.9 | 1.9 | 1.0 | 0.7 | 10.8 | 4.3 |
| 2322 | 898.8 | 126.1 | 72.6 | 38.6 | 28.5 | 26.9 | 7.1 | 2.7 | 1.4 | 1.1 | 12.4 | 4.7 |
| 2323 | 784.4 | 153.7 | 109.5 | 67.0 | 47.6 | 73.9 | 5.1 | 1.5 | 0.9 | 0.6 | 7.2 | 2.1 |
| 2324 | 526.6 | 99.7 | 44.4 | 22.4 | 17.0 | 18.8 | 5.3 | 2.4 | 1.2 | 0.9 | 11.9 | 5.3 |
| | | | | | | \bar{x} | 5.6 | 2.1 | 1.1 | 0.8 | 10.5 | 4.1 |

373 *Pfaf*: Pfafstetter code from HydroBASINS; *St*: Strahler order; *FR*: local French model; *EU*:
 374 global model at the European scale; *HCP_l*: HCP length *l* weighting; *HCP_v*: HCP volume *v*
 375 weighting



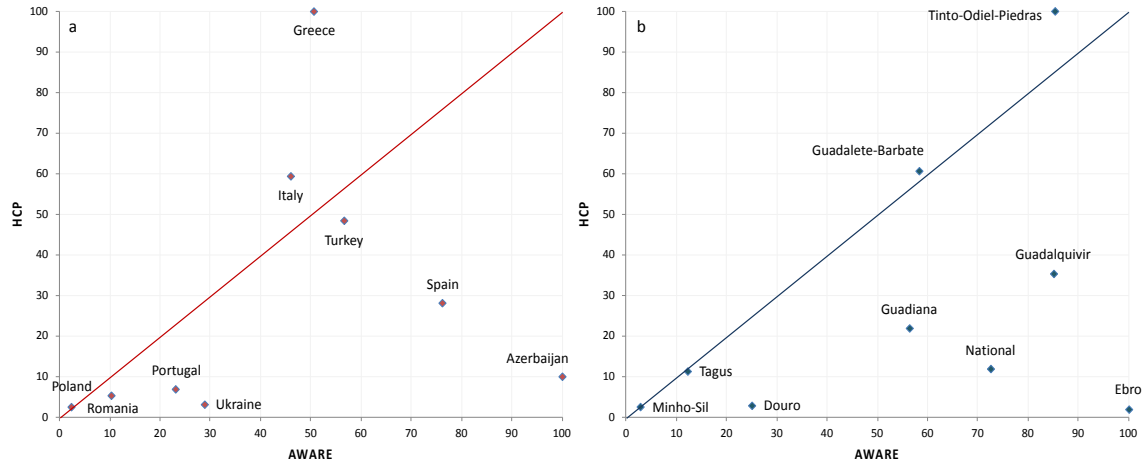
376
 377 **Figure 6.** Characterization factors for European watersheds with the detail of French watersheds
 378 HCP calculated using the generalized (July) and the local model (Q90), including high order
 379 streams

380 3.4 HCP and AWARE for agricultural water use

381 When comparing AWARE and HCP it should be kept in mind that indicator units are not the
382 same. While AWARE CFs are dimensionless, the HCP model quantifies the potential alteration in
383 habitat surface (m^2) for marginal discharge change (m^3/s). At country scale, the most evident
384 difference between both characterization approaches depicted in Figure 7a is the country where
385 consuming 1 m^3 of water for agriculture has the greatest impact. AWARE indicates Azerbaijan as
386 the most impacted country, while the highest HCP is attributed to Greece. This is due to intrinsic
387 differences of both models. AWARE represents available water remaining net of water demand
388 by humans and ecosystems (Boulay et al., 2018). As a result, high surface water demand in
389 Azerbaijan (SI, Table S4) is likely to increase the AWARE score compared to countries where
390 human water demand is less intense. On the contrary, HCP indicates habitat sensitivity to water
391 consumption regardless of the use and it is rather dependent on topographical and climatic
392 conditions. CF for Greece appears therefore higher and heavily influenced by HCP of insular areas
393 (e.g. Figure 4 and Figure 5). When the water mix is not taken into account and the impact is
394 allocated on all water sources indifferently, outcomes for Greece are closer in both models (SI,
395 Figure S2). In Ukraine, a relatively large water demand is the main reason for the difference
396 between AWARE and the HCP score, according to which stream habitats appear to be less
397 sensitive to consumptive water use.

398 When corresponding inventory data are available, impact assessment can be brought to
399 watershed level as illustrated in Figure 7b. The same concept discussed above applies to Spanish
400 river basins where the Ebro is the most stressed according to AWARE and the Tinto-Odiel-Piedras
401 catchment shows the highest habitat sensitivity. The HCP value for the Ebro stimulates reflection
402 on the spatial scales used for HCP aggregation. Values for the Ebro, as well as for other sensitive

403 Spanish river basins such as the Jucar or the Segura included in Figure 4, were averaged with reach
 404 characterization factors of Southern France at HB04 scale (Figure 5). In critical regions, a narrower
 405 spatial resolution could be beneficial to catch the detail of particularly vulnerable watersheds that
 406 would otherwise be lost using large scale characterization factors.
 407



408
 409 **Figure 7.** Impact of 1 m³ consumption of surface water for agriculture according to AWARE and
 410 HCP characterization models at a) country level and b) watershed scale in Spain

411 **4. CONCLUSIONS AND RESEARCH OUTLOOK**

412 Impact assessment of water consumption through habitat change potential modeling on
 413 individual river segments represents an advancement in terms of environmental relevance and
 414 spatial resolution of water consumption LCIA models. This study demonstrates the transferability
 415 of a high-resolution local HCP model at the continental scale and the validity of the chosen
 416 approach. The new model can be used to develop global characterization factors. Results at reach
 417 scale highlighted the importance of including small streams in the assessment, since they are the
 418 most sensitive to water volume change, and the habitats they harbor are therefore more likely to
 419 be affected by consumptive water use.

420 Even if LCA inventories frequently do not support this level of detail, high-resolution
421 characterization could highlight the uncertainty derived from ignoring spatial variability when
422 characterizing at lower spatial resolution. On the other hand, if spatially resolved inventory data
423 are used lower uncertainty could be achieved.

424 In order to facilitate the operationalization of the generalized HCP model, aggregation at
425 watershed has been carried out. However, in regions where HCP at reach is higher, a more refined
426 spatial resolution is preferable. On the contrary, for large watersheds in less vulnerable regions,
427 for instance in Central European river basins, a high level of detail would probably be excessive
428 and counter-productive in terms of inventory data availability. To allow applicability of the HCP
429 model in the short-term, country HCPs can be easily calculated and, even if important details at
430 the watershed scale may be missing, results can be compared with those deriving from existing
431 models such as AWARE. In addition, some interesting differences were highlighted between both
432 models demonstrating the interest of HCP characterization as a complementary indicator focused
433 specifically on assessing impacts on freshwater habitats.

434 The importance of linking inventory data and impact assessment refers as well to the
435 characterization of water consumption from a temporal point of view. For instance, in the example
436 discussed above, annual average CFs were associated to annual WSmix. Monthly CFs are
437 available, but the same detail is not provided by current water consumption data in inventories.
438 Moreover, reservoir water has been included in generic surface water consumption. However,
439 reservoirs can be used to ensure sufficient supply of water volumes needed for human activities
440 and ecosystems in dry season, mitigating water shortage in downstream rivers, which is not taken
441 into account in current models (neither in AWARE nor in the HCP model). Nonetheless, river

442 regulation and inter-basin transfer may involve non-marginal changes in river environmental and
443 ecological conditions that would not be covered by the HCP model as it is.

444 Concerning the temporally resolved assessment of HCP, it should also be considered that the
445 HCP model does not apply to all flow magnitudes. Consequences of a high flow period on
446 freshwater habitats are different than during low flows. Calculating monthly HCP has been
447 necessary because it is not possible to define locally when low and high flows occur. However,
448 monthly discharges used to compute HCP can be still considered averages and therefore high flow
449 peaks are flattened. An alternative to modeling monthly CF would be to derive median and
450 minimum discharge for each river segment as a proxy for Q_{50} and Q_{90} , and use the resulting HCP
451 for the wet and the dry season respectively, as done in Damiani et al. (2019). This solution could
452 also be compared with HCPs from average and minimum discharge modeled in other existing
453 databases (e.g. Linke et al., 2019). Notwithstanding, the HCP value for high discharge is extremely
454 low and yet likely to be overestimated because deriving from fitting a model on median and low
455 flow HCPs. In addition, given the temporal resolution of HCP being monthly, this is not likely to
456 occur frequently, assuming high flow peaks do not tend to last longer than a couple of weeks.
457 Furthermore, inventory data are currently not likely to reflect temporal resolutions beyond
458 trimestral or seasonal resolution and will in most cases be annual averages. Uncertainty deriving
459 from including potential high flow periods in the characterization is therefore likely to be
460 negligible in practice.

461 It is also important to mention that water consumption LCA could fully take advantage of
462 temporal and spatial quantification of water consumption inventory data and impact
463 characterization, only if inventory and effects are linked by a mechanistic fate factor describing

464 water balance variations in different environmental compartments following withdrawal (e.g.
465 aquifer, river, soil; Núñez et al., 2018).

466 As a long-term perspective, a mechanistic pathway linking water consumption to a fate factor
467 and an effect factor based on HCP allows reach-scale, mechanistic, endpoint impact modeling
468 when combined with information on the biological context at the reach scale. This could include
469 the presence or absence of species or functional guilds adapted to a certain hydraulic habitat
470 (considering also their economic, social, and cultural values). A reduction in river discharge in dry
471 months results in lower average Reynolds number in river reaches and in higher HCP for those
472 habitats, and therefore those species, more vulnerable to water volume alteration. Ecohydrological
473 habitat models at the root of the HCP model are derived from empirical, species abundance data.
474 Relating habitat availability to predicted sensitive species abundance and density, which is
475 currently subject of extensive research (Lamouroux and Olivier, 2015; Méricoux et al., 2015),
476 could allow developing LCIA indicators of potential abundance when hydraulics is the limiting
477 factor. In addition, regarding hydraulic modeling of river habitat, width and depth equations used
478 in the present study are discharge dependent but can be improved including geomorphological
479 variables, as for instance catchment slopes, geology or landcover (Morel et al., 2020).

480 With the purpose of developing global endpoint models based on freshwater habitat change
481 potential, it is even more crucial to define the range of validity of the model. In the present study,
482 HCP values greater than $25\ 000\ \text{m}^2\ \text{s}/\text{m}^3$ were excluded. These were mostly associated with streams
483 in arid and desert regions that are most likely characterized by ecological conditions different from
484 those on which the HCP model is based. These rivers are predominantly intermittent and identified
485 calculating discharge at monthly resolution. A better, global characterization of intermittent
486 streams from a hydrologic and ecological perspective would certainly improve the applicability of

487 the model in the most arid areas. To limit HCP outliers, the possibility to apply the model on a
488 minimum discharge threshold could also be investigated, based on hydrology, water users,
489 demographics, or water management policies adopted in certain regions.

490 It should also be considered that the generalized model has been developed based on local HCP
491 calculated using habitat preference equations for species that are not ubiquitous. However, it is
492 assumed that hydrological and hydraulic conditions within validity of the HCP model would
493 globally determine the establishment of comparable habitats and the presence (or absence) of
494 species with convergent behavior and habitat preferences (Lamouroux et al., 2002), allowing to
495 define species archetypes to apply the HCP model at the global level for midpoint and endpoint
496 LCIA.

497 **ASSOCIATED CONTENT**

498 A Supporting Information document is available including:

- 499 • statistics on modeled streamflow values and HCPs;
- 500 • HCP monthly maps;
- 501 • data used for the AWARE and HCP model comparison.

502 **ACKNOWLEDGEMENTS**

503 The authors are grateful to all members of the ELSA research group for their advice
504 (Environmental Life Cycle and Sustainability Assessment, <http://www.elsa-lca.org/>). The authors
505 acknowledge ANR, the Occitanie Region, ONEMA and the industrial partners (BRL, SCP, SUEZ
506 Groupe, VINADEIS, Compagnie Fruitière) for the financial support of the Industrial Chair for
507 Environmental and Social Sustainability Assessment “ELSA-PACT” (grant no. 13-CHIN-0005-
508 01).

509 **REFERENCES**

- 510 Alcamo, J., Döll, P., Henrichs, T., Kaspar, F., Lehner, B., Rösch, T., Siebert, S., 2003.
511 Development and testing of the WaterGAP 2 global model of water use and availability.
512 Hydrol. Sci. J. 48, 317–337. <https://doi.org/10.1623/hysj.48.3.317.45290>
- 513 Andreadis, K.M., Schumann, G.J.P., Pavelsky, T., 2013. A simple global river bankfull width and
514 depth database. Water Resour. Res. 49, 7164–7168. <https://doi.org/10.1002/wrcr.20440>
- 515 Barbarossa, V., Huijbregts, M.A.J., Hendriks, A.J., Beusen, A.H.W., Clavreul, J., King, H.,
516 Schipper, A.M., 2017. Developing and testing a global-scale regression model to quantify
517 mean annual streamflow. J. Hydrol. 544, 479–487.
518 <https://doi.org/10.1016/j.jhydrol.2016.11.053>
- 519 Boulay, A.-M., Bare, J., Benini, L., Berger, M., Lathuillière, M., Manzardo, A., Margni, M.,
520 Motoshita, M., Núñez, M., Pastor, A. V., Ridoutt, B., Oki, T., Worbe, S., Pfister, S., 2018.
521 The WULCA consensus characterization model for water scarcity footprints: Assessing
522 impacts of water consumption based on available water remaining (AWARE). Int. J. Life
523 Cycle Assess. 23, 368–378. <https://doi.org/10.1007/s11367-017-1333-8>
- 524 Conrad, O., Bechtel, B., Bock, M., Dietrich, H., Fischer, E., Gerlitz, L., Wehberg, J., Wichmann,
525 V., Böhner, J., 2015. System for Automated Geoscientific Analyses (SAGA) v. 2.1.4. Geosci.
526 Model Dev. 8, 1991–2007. <https://doi.org/10.5194/gmd-8-1991-2015>
- 527 Dalin, C., Wada, Y., Kastner, T., Puma, M.J., 2017. Groundwater depletion embedded in
528 international food trade. Nature 543, 700–704. <https://doi.org/10.1038/nature21403>
- 529 Damiani, M., Lamouroux, N., Pella, H., Roux, P., Loiseau, E., Rosenbaum, R.K., 2019. Spatialized

530 freshwater ecosystem life cycle impact assessment of water consumption based on instream
531 habitat change modeling. *Water Res.* 163, 1–12.
532 <https://doi.org/10.1016/j.watres.2019.114884>

533 Damiani, M., Roux, P., Núñez, M., Loiseau, E., Rosenbaum, R.K., 2018. Addressing water needs
534 of freshwater ecosystems in life cycle impact assessment of water consumption : state of the
535 art and applicability of ecohydrological approaches to ecosystem quality characterization. *Int.*
536 *J. Life Cycle Assess.* 23, 2071–2088. [https://doi.org/https://doi.org/10.1007/s11367-017-](https://doi.org/10.1007/s11367-017-1430-8)
537 1430-8

538 Döll, P., Kaspar, F., Lehner, B., 2003. A global hydrological model for deriving water availability
539 indicators: Model tuning and validation. *J. Hydrol.* 270, 105–134.
540 [https://doi.org/10.1016/S0022-1694\(02\)00283-4](https://doi.org/10.1016/S0022-1694(02)00283-4)

541 European Environment Agency, 2018. EEA Signals 2018 — Water is life, Eea Signals.
542 Publications Office of the European Union, Copenhagen. <https://doi.org/10.2800/52469>

543 Fick, S.E., Hijmans, R.J., 2017. WorldClim 2: new 1-km spatial resolution climate surfaces for
544 global land areas. *Int. J. Climatol.* 37, 4302–4315. <https://doi.org/10.1002/joc.5086>

545 Hanafiah, M.M., Xenopoulos, M. a, Pfister, S., Leuven, R.S.E.W., Huijbregts, M. a J., 2011.
546 Characterization factors for water consumption and greenhouse gas emission based on
547 freshwater fish species extinction. *Environ. Sci. Technol.* 45, 5272–5278.

548 Hubert, M., Vandervieren, E., 2008. An adjusted boxplot for skewed distributions. *Comput. Stat.*
549 *Data Anal.* 52, 5186–5201. <https://doi.org/10.1016/j.csda.2007.11.008>

550 Janse, J.H., Kuiper, J.J., Weijters, M.J., Westerbeek, E.P., Jeuken, M.H.J.L., Bakkenes, M.,

551 Alkemade, R., Mooij, W.M., Verhoeven, J.T.A., 2015. GLOBIO-Aquatic, a global model of
552 human impact on the biodiversity of inland aquatic ecosystems. *Environ. Sci. Policy* 48, 99–
553 114. <https://doi.org/10.1016/j.envsci.2014.12.007>

554 Lamouroux, N., Capra, H., 2002. Simple predictions of instream habitat model outputs for target
555 fish populations. *Freshw. Biol.* 47, 1543–1556. <https://doi.org/10.1046/j.1365-2427.2002.00879.x>

557 Lamouroux, N., Olivier, J.M., 2015. Testing predictions of changes in fish abundance and
558 community structure after flow restoration in four reaches of a large river (French Rhône).
559 *Freshw. Biol.* 60, 1118–1130. <https://doi.org/10.1111/fwb.12324>

560 Lamouroux, N., Poff, N.L., Angermeier, P.L., 2002. Intercontinental Convergence of Stream Fish
561 Community Traits Along Geomorphic and Hydraulic Gradients. *Ecology* 83, 1792–1807.
562 [https://doi.org/10.1890/0012-9658\(2002\)083\[1792:ICOSFC\]2.0.CO;2](https://doi.org/10.1890/0012-9658(2002)083[1792:ICOSFC]2.0.CO;2)

563 Lamouroux, N., Souchon, Y., 2002. Simple predictions of instream habitat model outputs for fish
564 habitat guilds in large streams. *Freshw. Biol.* 47, 1531–1542. <https://doi.org/10.1046/j.1365-2427.2002.00879.x>

566 Leão, S., Roux, P., Núñez, M., Loiseau, E., Junqua, G., Sferratore, A., Penru, Y., Rosenbaum,
567 R.K., 2018. A worldwide-regionalised water supply mix (WSmix) for life cycle inventory of
568 water use. *J. Clean. Prod.* 172, 302–313.
569 <https://doi.org/https://doi.org/10.1016/j.jclepro.2017.10.135>

570 Lehner, B., Grill, G., 2013. Global river hydrography and network routing: baseline data and new
571 approaches to study the world’s large river systems. *Hydrol. Process.* 27, 2171–2186.

572 <https://doi.org/10.1002/hyp.9740>

573 Leigh, C., Boulton, A.J., Courtwright, J.L., Fritz, K., May, C.L., Walker, R.H., Datry, T., 2016.
574 Ecological research and management of intermittent rivers: an historical review and future
575 directions. *Freshw. Biol.* 61, 1181–1199. <https://doi.org/10.1111/fwb.12646>

576 Leopold, L.B., Maddock, T., 1953. *The Hydraulic Geometry of Stream Channels and Some*
577 *Physiographic Implications*, Geological Survey Professional Paper 252. Washington, DC.

578 Linke, S., Lehner, B., Dallaire, C.O., Ariwi, J., Grill, G., Anand, M., Beames, P., Burchard-levine,
579 V., Moidu, H., Tan, F., Thieme, M., 2019. HydroATLAS : global hydro-environmental sub-
580 basin and river reach characteristics at high spatial resolution 0–25.
581 <https://doi.org/10.1038/s41597-019-0300-6>

582 Loiseau, E., Aissani, L., Le Féon, S., Laurent, F., Cerceau, J., Sala, S., Roux, P., 2018. Territorial
583 Life Cycle Assessment (LCA): What exactly is it about? A proposal towards using a common
584 terminology and a research agenda. *J. Clean. Prod.* 176, 474–485.
585 <https://doi.org/10.1016/j.jclepro.2017.12.169>

586 Méricoux, S., Forcellini, M., Dessaix, J., Fruget, J.F., Lamouroux, N., Statzner, B., 2015. Testing
587 predictions of changes in benthic invertebrate abundance and community structure after flow
588 restoration in a large river (French Rhône). *Freshw. Biol.* 60, 1104–1117.
589 <https://doi.org/10.1111/fwb.12422>

590 Moran, D., Kanemoto, K., 2017. Identifying the Species Threat Hotspots from Global Supply
591 Chains. *Nat. Ecol. Evol.* 1, 1–5. <https://doi.org/doi:10.1038/s41559-016-0023>

592 Morel, M., Booker, D.J., Gob, F., Lamouroux, N., 2020. Intercontinental predictions of river

593 hydraulic geometry from catchment physical characteristics. *J. Hydrol.* 582, 124292.
594 <https://doi.org/10.1016/j.jhydrol.2019.124292>

595 Nitschelm, L., Aubin, J., Corson, M.S., Viaud, V., Walter, C., 2016. Spatial differentiation in Life
596 Cycle Assessment LCA applied to an agricultural territory: Current practices and method
597 development. *J. Clean. Prod.* 112, 2472–2484. <https://doi.org/10.1016/j.jclepro.2015.09.138>

598 Núñez, M., Bouchard, C.R., Bulle, C., Boulay, A.M., Margni, M., 2016. Critical analysis of life
599 cycle impact assessment methods addressing consequences of freshwater use on ecosystems
600 and recommendations for future method development. *Int. J. Life Cycle Assess.* 21, 1799–
601 1815. <https://doi.org/10.1007/s11367-016-1127-4>

602 Núñez, M., Rosenbaum, R.K., Karimpour, S., Boulay, A.-M., Lathuillière, M.J., Margni, M.,
603 Scherer, L., Verones, F., Pfister, S., 2018. A multimedia hydrological fate modelling
604 framework to assess water consumption impacts in Life Cycle Assessment. *Environ. Sci.*
605 *Technol.* 52, 4658–4667. <https://doi.org/10.1021/acs.est.7b05207>

606 Palmer, M.A., Lettenmaier, D.P., Poff, N.L., Postel, S.L., Richter, B., Warner, R., 2009. Climate
607 change and river ecosystems: Protection and adaptation options. *Environ. Manage.* 44, 1053–
608 1068. <https://doi.org/10.1007/s00267-009-9329-1>

609 Park, C.C., 1977. World-wide variations in hydraulic geometry exponents of stream channels: an
610 analysis and some observations. *J. Hydrol.* 33, 133–146. [https://doi.org/10.1016/0022-1694\(77\)90103-2](https://doi.org/10.1016/0022-1694(77)90103-2)

612 Pastor, A. V., Ludwig, F., Biemans, H., Hoff, H., Kabat, P., 2014. Accounting for environmental
613 flow requirements in global water assessments. *Hydrol. Earth Syst. Sci.* 18, 5041–5059.

614 <https://doi.org/10.5194/hess-18-5041-2014>

615 Pekel, J., Cottam, A., Gorelick, N., Belward, A.S., 2016. High-resolution mapping of global
616 surface water and its long-term changes. *Nature* 540, 418–422.
617 <https://doi.org/10.1038/nature20584>

618 Pella, H., Lejot, J., Lamouroux, N., Snelder, T., 2012. Le réseau hydrographique théorique (RHT)
619 français et ses attributs environnementaux. *Géomorphologie Reli. Process. Environ.* 18, 317–
620 336. <https://doi.org/10.4000/geomorphologie.9933>

621 Pfister, S., Koehler, A., Hellweg, S., 2009. Assessing the environmental impacts of freshwater
622 consumption in LCA. *Environ. Sci. Technol.* 43, 4098–4104.
623 <https://doi.org/10.1021/es802423e>

624 Quantum GIS Development Team, 2017. Quantum GIS Geographic Information System.

625 R Core Team, 2016. R: A language and environment for statistical computing.

626 Rhodes, D.D., 1978. World-wide variations in hydraulic geometry exponents of stream channels:
627 an analysis and some observations — comments 39, 193–197. [https://doi.org/10.1016/0022-](https://doi.org/10.1016/0022-1694(78)90123-3)
628 [1694\(78\)90123-3](https://doi.org/10.1016/0022-1694(78)90123-3)

629 RStudio Team, 2016. RStudio: integrated development environment for R.

630 Tendall, D.M., Hellweg, S., Pfister, S., Huijbregts, M. a J., Gaillard, G., 2014. Impacts of river
631 water consumption on aquatic biodiversity in life cycle assessment - a proposed method, and
632 a case study for Europe. *Environ. Sci. Technol.* 48, 3236–44.
633 <https://doi.org/10.1021/es4048686>

634 UNESCO, UN-Water, 2020. The United Nations World Water Development Report 2020: Water
635 and Climate Change. Paris.

636 Verones, F., Pfister, S., Hellweg, S., 2013a. Quantifying area changes of internationally important
637 wetlands due to water consumption in LCA. *Environ. Sci. Technol.* 47, 9799–9807.
638 <https://doi.org/10.1021/es400266v>

639 Verones, F., Pfister, S., van Zelm, R., Hellweg, S., 2017. Biodiversity impacts from water
640 consumption on a global scale for use in life cycle assessment. *Int. J. Life Cycle Assess.* 22,
641 1247–1256. <https://doi.org/10.1007/s11367-016-1236-0>

642 Verones, F., Saner, D., Pfister, S., Baisero, D., Rondinini, C., Hellweg, S., 2013b. Effects of
643 consumptive water use on biodiversity in wetlands of international importance. *Environ. Sci.*
644 *Technol.* 47, 12248–12257. <https://doi.org/10.1021/es403635j>

645 Vörösmarty, C.J., McIntyre, P.B., Gessner, M.O., Dudgeon, D., Prusevich, A., Green, P., Glidden,
646 S., Bunn, S.E., Sullivan, C.A., Liermann, C.R., Davies, P.M., 2010. Global threats to human
647 water security and river biodiversity. *Nature* 467, 555–561.
648 <https://doi.org/doi:10.1038/nature09440>

649 Vörösmarty, C.J., Pahl-Wostl, C., Bunn, S.E., Lawford, R., 2013. Global water, the anthropocene
650 and the transformation of a science. *Curr. Opin. Environ. Sustain.* 5, 539–550.
651 <https://doi.org/10.1016/j.cosust.2013.10.005>

652